Canonical Correlation Forests

Tom Rainforth and Frank Wood

Abstract—We introduce canonical correlation forests (CCFs), a new decision tree ensemble method for classification. Individual canonical correlation trees are binary decision trees with hyperplane splits based on canonical correlation components. Unlike axis-aligned alternatives, the decision surfaces of CCFs are not restricted to the coordinate system of the input features and therefore more naturally represent data with correlation between the features. Additionally we introduce a novel alternative to bagging, the projection bootstrap, which maintains use of the full dataset in selecting split points. CCFs do not require parameter tuning and our experiments show that they out-perform axis-aligned random forests, other state-of-the-art tree ensemble methods and all of the 179 classifiers considered in a recent extensive survey.

1 Introduction

Decision tree ensemble methods such as random forests [1], extremely randomized trees [2] and boosted decision trees [3] are widely employed methods for classification and regression due to their scalability, fast out of sample prediction, and tendency to require little parameter tuning. In many cases, they are capable of giving predictive performance close to, or even equalling, state of the art when used in an out-of-the-box fashion. The trees used in such models are, however, typically axis-aligned, restricting the ensemble decision surface to be piecewise axis-aligned, even when there is little evidence for this in the data. Canonical correlation forests (CCFs) overcome this problem by instead using carefully chosen hyperplane splits, leading to a more powerful classifier that naturally incorporates correlation between the features, as shown in Figure 1. In this paper we demonstrate that this innovation regularly leads to a significant increase in accuracy over previous state-of-the-art tree ensemble methods, whilst maintaining speed and black-box applicability. Furthermore, we demonstrate that CCFs run without parameter tuning outperform all of the 179 classifiers considered in the recent survey of Fernández-Delgado et al [4] over a large selection of datasets, including many popular support vector machines and neural nets.

A decision tree is a predictive model that imposes sequential divisions of an input space to form a set of partitions known as leafs, each containing a local classification or regression model. Out of sample prediction is performed by using the partitioning structure to assign a data point to a particular leaf and then using the corresponding local predictive model. Typically, the leaf models are taken to be independent of each other and the class labels are assumed to be independent of input features given the leaf assignments.

Classical decision tree learning algorithms work in a greedy top down fashion, exhaustively searching the possible space of axis-aligned unique split points and choosing the best based on a splitting criterion, such as the Gini gain or information gain used in CART [5] and C4.5 [6] respectively. This process continues until no further split is advantageous or some user-set limit is reached. For classification with continuous features this typically only occurs once each leaf is "pure," containing only data points of a single class. When used as individual classifiers, trees are usually "pruned" after being grown to prevent overfitting.

• *Tom Rainforth and Frank Wood are with the Department of Engineering Science, University of Oxford (e-mail: {twgr, fwood}@robots.ox.ac.uk)*

It was established by Ho [7] that combining individual trees to form a decision forest can simultaneously improve predictive performance and provide regularization against over-fitting, with the need for pruning. In a forest, each tree is separately trained, with predictions based on a voting system across the ensemble. As classical decision tree algorithms are deterministic procedures, such combination requires the introduction of probabilistic elements into the generative process to prevent identical trees. The random subspace method used by Ho (refined in a later paper [8]) involves only searching splits along a randomly selected subset of the features at each node. Breiman [9] proposed the alternative scheme of bagging, in which each predictor is trained on a bootstrap sample of the original dataset. Breiman later combined these schemes to great effect in his popular random forest (RF) algorithm [1]. He also demonstrated that splitting along random linear combinations of features at each node can give small performance improvements over using a single feature.

Oblique decision trees (ODTs) extend classical decision trees by splitting using linear combinations of the available features. Some algorithms such as OC1 [10] attempt to directly optimize for the hyperplane representing the best partition, while others, such as functional trees [11] and QUEST [12], carry out a linear discriminant analysis (LDA) to find a projection which optimizes some discriminant criterion and then search over possible splits in this projected space. Although ODTs generally produce better results than single axis aligned trees, existing algorithms suffer from a number of common issues, such as a failure to effectively deal with multiple classes, numerical instability or significant increase in computational cost. Most also carry out a simplified version of Fisher's LDA [13], making the unnecessary assumptions that the classes are normally distributed with the same covariance.

Lemmond et al [14] and Menze et al [15] both introduce the idea of creating forests of oblique decision trees using splits based on LDA projections. However, neither method is applicable to multi-class classification and neither carries out the LDA in a manner that is both numerically stable and computationally efficient. The latter paper also introduce the idea of carrying out LDA as a ridge regression, where there is regularization towards the principle component directions. However, their results suggest no advantage is gained by this regularization.

Rotation forests [16] use individually orthogonal trees, but apply probabilistic rotations, based on principle component analysis, to the original coordinate system as a preprocessing step, such

(a) Single CART (unpruned) (b) RF with 200 Trees (c) Single CCT (unpruned) (d) CCF with 200 Trees

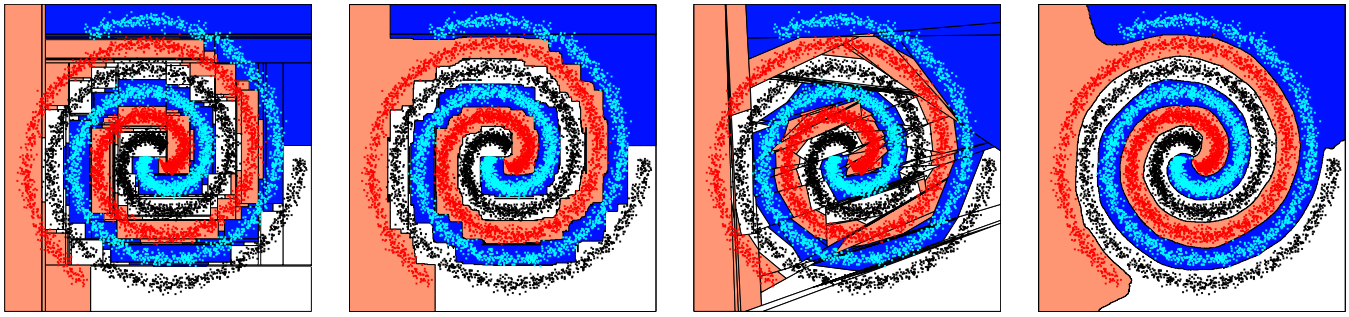

Fig. 1: Decision surfaces for artificial spirals dataset. (a) Shows the hierarchical partitions and surface for a single axis aligned tree while (b) shows the effect of averaging over a number of, individually randomized, axis aligned trees. (c) Shows a single canonical correlation tree (CCT) and (d) demonstrates that averaging over CCTs to give a canonical correlation forest leads to "smoother" decision surfaces which better represent the data than the axis aligned equivalent.

that different trees are trained in a different coordinate system. Although this was shown to given significant improvement in predictive performance over RF, they require all features to be considered for splitting at every node, leading to a computationally relatively expensive algorithm for more than a modest number of features.

2 Canonical Correlation Forests

Canonical correlation forests (CCFs) are a new tree ensemble method for classification. Individual canonical correlation trees (CCTs) are oblique decision trees, trained by using canonical correlation analysis (CCA) [17] to find feature projections that give the maximum correlation between the features and a coordinate free representation of the class labels, and then selecting the best split in this projected space. Unlike many previous oblique forest methods, CCFs are equally suited to both binary and multi-class classification, have the same computational complexity as RFs and calculate the splitting hyperplanes in a numerically stable manner. We also introduce the projection bootstrap, a novel alternative to bagging. Open source code for CCFs is available online[1]. Both training and testing of the algorithm require only a single short line of code without the need for parameter tuning (although there are a small number of parameter which can be changed, all presented results are created using default values).

2.1 Forest Definition and Notation

Although the model we introduce can easily be extended to regression problems, our focus will be on classification. Our aim will be to predict class labels $y_n \in \{1, \ldots, K\}$ given a vector of input features $x_n \in \mathbb{R}^D$ for each data point $n \in \{1, \ldots, N\}$. We will denote the set of labels $Y = \{y_n\}_{n=1}^N$ and the set of feature vectors $X = \{x_n\}_{n=1}^N$. Let $T = \{t_i\}_{i=1\ldots L}$ denote a forest comprised of binary trees t_i, where L is a user set parameter dictating the ensemble size. The model operates in a train / test fashion, in which T is learnt using training data and out of sample predictions are made independently of the training data conditioned on T. Each individual tree $t = \{\Psi, \Theta\}$ is defined by a set of discriminant nodes $\Psi = \{\psi_j\}_{j \in \mathcal{J} \setminus \partial\mathcal{J}}$ and a set of leaf nodes $\Theta = \{\theta_j\}_{j \in \partial\mathcal{J}}$ where $\mathcal{J} \subset \mathbb{Z}^{\geq 0}$ is a set of node indices and $\partial\mathcal{J} \subseteq \mathcal{J}$ is the subset of leaf node indices. Each discriminant node is defined by the tuple $\psi_j = \{\chi_{j,1}, \chi_{j,2}, \phi_j, s_j\}$ where $\{\chi_{j,1}, \chi_{j,2}\} \subseteq \mathcal{J} \setminus j$ are the two child node ids, $\phi_j \in \mathbb{R}^D$ is a weight vector used to project the input features and s_j is the point at which the splitting occurs in the projected space $X^T\phi_j$. Note that for orthogonal trees only a single element of ϕ_j will be non-zero, whereas oblique trees will have multiple non-zero elements. Let $B(j,t)$ denote the partition of the input space associated with node j such that $B(0,t) = \mathbb{R}^D$ and $B(j,t) = B(\chi_{j,1},t) \cup B(\chi_{j,2},t)$. The partitioning procedure is then defined such that

$$\begin{aligned} B(\chi_{j,1},t) &= B(j,t) \cap \left\{ z \in \mathbb{R}^D : z^T\phi_j \leq s_j \right\} \\ B(\chi_{j,2},t) &= B(j,t) \cap \left\{ z \in \mathbb{R}^D : z^T\phi_j > s_j \right\}. \end{aligned} \tag{1}$$

Thus Ψ defines a hierarchical partitioning procedure that deterministically assigns data points to leaf nodes, with prediction then based on the corresponding local leaf model. Although more complicated leaf models are possible (e.g. logistic regression models [11]), in this paper we only consider the case where the leaf models are deterministic assignments to a particular class, thus $\theta_j \in \{1, \ldots, K\}\ \forall j \in \partial\mathcal{J}$.

As for RFs, out of sample prediction is done using an equally weighted voting scheme of the tree predictions. The predictive probability assigned to a certain class is thus the number of trees that predicted that class divided by the total number of trees.

2.2 Canonical Correlation Analysis

Canonical correlation analysis (CCA) [17] is a deterministic method giving of pairs of linear projections that maximise the correlation between two matrices in the co-projected space. Let us consider applying CCA between the arbitrary matrices $W \in \mathbb{R}^{n \times d}$ and $V \in \mathbb{R}^{n \times k}$, and let $a \in \mathbb{R}^{d \times 1}$, $\|a\|_2 = 1$ and $b \in \mathbb{R}^{k \times 1}$, $\|b\|_2 = 1$ be arbitrary vectors on the $(d-1)$-hypersphere and $(k-1)$-hypersphere respectively. Denote the set of solutions for the canonical coefficients as $\{A_\nu, B_\nu\}_{\nu \in \{1,\ldots,\nu_{max}\}}$ where each A_ν and B_ν are in the space of a and b respectively and $\nu_{\max} = \min(\text{rank}(W), \text{rank}(V))$. The first pair of canonical coefficients are given by

$$\{A_1, B_1\} = \underset{a,b}{\text{argmax}} \left(\text{corr}(Wa, Vb) \right) \tag{2}$$

and the corresponding canonical correlation components are given by WA_1 and VB_1. The second pair of coefficients, $\{A_1, B_1\}$ is

1. http://www.robots.ox.ac.uk/~twgr/

Algorithm 1: CCF training algorithm

Inputs: ordinal features $X^r \in \mathbb{R}^{N\times D^r}$, categorical features $X^c \in \mathcal{S}^{N\times D^c}$, class labels $\mathcal{Y} \in \mathbb{I}^{N\times K}$, number of trees $L \in \mathbb{Z}^+$, number of features to sample $\lambda \in \{1,\dots,D^r+D^c\}$
Outputs: CCF T

Convert X^c to 1-of-K encoding $X^b \in \mathbb{I}^{N\times D^b}$
$X = \left\{X^r, X^b\right\}$
$\mu_{(d)} = \sum_{n=1}^{N} X_{(n,d)}/N \quad \forall d$
$\sigma_{(d)} = \left(\frac{1}{N-1}\sum_{n=1}^{N} {X_{(n,d)}}^2 - {\mu_{(d)}}^2\right)^{0.5} \quad \forall d$
$X_{(:,d)} \leftarrow \left(X_{(:,d)} - \mu_{(d)}\right)/\sigma_{(d)} \quad \forall d$
Set missing values in X to 0
if $\lambda < (D^r + D^c)$ **then** $b = \text{true}$ **else** $b = \text{false}$ **end if**
for $i = 1\colon L$ **do**
  if b **then**
    $\{X', \mathcal{Y}'\} \leftarrow \{X, \mathcal{Y}\}$
  else
    $\{X', \mathcal{Y}'\} \leftarrow$ bootstrap sample N rows from $\{X, \mathcal{Y}\}$
  end if
  $[\cdot, \Psi, \Theta] = \text{GROWTREE}(X', \mathcal{Y}', \{1,\dots,D^r+D^c\}, \lambda, b)$
  $t_i = \{\Psi, \Theta\}$
end for
return $T = \{t_i\}_{i=1\dots L}$

given by the solution to (2) under the additional constraint that new components are uncorrelated with the previous components:

$$(WA_1)^T WA_2 = 0 \quad \text{and} \quad (VB_1)^T VB_2 = 0. \tag{3}$$

This process is repeated with all new components uncorrelated with the previous components, to produce a full set of ν_{max} pairs of canonical coefficients. Note that CCA is a co-ordinate free process that is unaffected by rotation, translation or global scaling of the inputs.

As shown by, for example, Borga [18], the solution of CCA has a closed form. Namely the coefficients satisfy:

$$\begin{aligned}\Sigma_{WW}^{-1}\Sigma_{WV}\Sigma_{VV}^{-1}\Sigma_{VW}A_\nu &= \rho_\nu^2 A_\nu \\ \Sigma_{VV}^{-1}\Sigma_{VW}\Sigma_{WW}^{-1}\Sigma_{WV}B_\nu &= \rho_\nu^2 B_\nu\end{aligned} \tag{4}$$

where Σ_{WW}, Σ_{VV} and $\Sigma_{WV} = \Sigma_{VW}^T$ are the covariance of W, covariance of V and cross covariance of W and V respectively. The common eigenvalues, which correspond to the squares of the canonical correlations ρ_ν, make the pairing between the coefficients of W and V apparent and the order of the coefficients is found by the corresponding decreasing order of the canonical correlations, $\rho_1 \geq \rho_2 \geq \cdots \geq \rho_{\nu_{\max}}$.

2.3 Canonical Correlation Forest Training Algorithm

Algorithm 1 gives a step by step process for the generation of a CCF. We use $\leftarrow$ to denote assignment and MATLAB notation with subscript parentheses for indexing such that a colon indicates all the values along a dimension, a vector index indicates assignment to the corresponding subarray and the notation $:\backslash i$ indicates all the indices except those in set i.

CCTs are trained in the greedy, top down procedure shown in Algorithm 2. Note that this is self similar for sub-trees and continues until no split is beneficial. The key difference to classical decision learning tree algorithms is that instead of searching over the axis aligned splits, a CCA is first carried out between the features and classes and then the split is selected using an exhaustive search in the space of projected features.

Algorithm 2: GROWTREE

Inputs: features $X^j \in \mathbb{R}^{N^j\times\left(D^r+D^b\right)}$, classes $\mathcal{Y}^j \in \mathbb{I}^{N^j\times K}$, available feature ids $\mathcal{D}^j \subseteq \{1,\dots,D^r+D^c\}$, number of features to sample $\lambda \in \mathbb{Z}^+$, whether to projection bootstrap $b \in \{\text{true}, \text{false}\}$
Outputs: Sub-tree root node identifier j, sub-tree discriminant nodes Ψ, sub-tree leaf nodes Θ

Set current node index j to an unique node identifier
Sample $\delta \subseteq \mathcal{D}^j$ by taking $\min\left(\lambda, \left|\mathcal{D}^j\right|\right)$ samples without replacement from $\mathcal{D}^j$
While δ contains features without variation, eliminate these from $\mathcal{D}^j$ and δ and resample
$\gamma = \delta$ mapped to the column indices of X^j in accordance with the 1-of-K encoding of X^c
if b **then**
  $\{X', \mathcal{Y}'\} \leftarrow$ bootstrap sample N^j rows from $\{X^j_{(:,\gamma)}, \mathcal{Y}^j\}$
else
  $\{X', \mathcal{Y}'\} \leftarrow \{X, \mathcal{Y}\}$
end if
if all rows in X' or $\mathcal{Y}'$ are identical **then**
  if all rows in $X^j_{(:,\gamma)}$ or $\mathcal{Y}^j$ are identical **then**
    return $\left[j, \emptyset, \text{LABEL}(\mathcal{Y}^j)\right]$ ▷ LABEL as per Section 2.3
  end if
  $\{X', \mathcal{Y}'\} \leftarrow \{X^j_{(:,\gamma)}, \mathcal{Y}^j\}$
end if
if X' contains only two unique rows **then**
  $\mathcal{X}' = \text{UNIQUEROWS}(X')$
  $\phi_{j\,(\gamma)} \leftarrow \mathcal{X}'_{(2,:)} - \mathcal{X}'_{(1,:)}, \quad \phi_{j\,(:\backslash\gamma)} \leftarrow 0$
  $s_j = \frac{1}{2}\left(\mathcal{X}'_{(1,:)} + \mathcal{X}'_{(2,:)}\right)^T \phi_j$
else
  $[\Phi, \cdot] = \text{CCA}(X', \mathcal{Y}')$ ▷ as per Section 2.5
  $R_{(\gamma,:)} \leftarrow \Phi, \quad R_{(:\backslash\gamma,:)} \leftarrow 0$
  $U = X^j R$
  $[\xi, s_j, \text{gain}] = \text{FINDBESTSPLIT}(U)$ ▷ as per Section 2.3
  if gain ≤ 0 **then**
    return $\left[j, \emptyset, \text{LABEL}(\mathcal{Y}^j)\right]$
  end if
  $\phi_j = R_{(:,\xi)}$
end if
$\tau_l = \left\{n \in \left\{1,\dots,N^j\right\} : X^j_{(n,:)}\phi_j \leq s_j\right\}$
$\tau_r = \{1,\dots,N^j\}\backslash\tau_l$
$\left[\chi_{(j,1)}, \Psi_l, \Theta_l\right] = \text{GROWTREE}(X^j_{(\tau_l,:)}, \mathcal{Y}^j_{(\tau_l,:)}, \mathcal{D}^j, \lambda, b)$
$\left[\chi_{(j,2)}, \Psi_r, \Theta_r\right] = \text{GROWTREE}(X^j_{(\tau_r,:)}, \mathcal{Y}^j_{(\tau_r,:)}, \mathcal{D}^j, \lambda, b)$
$\psi_j = \left\{\chi_{(j,1)}, \chi_{(j,2)}, \phi_j, s_j\right\}$
return $[j, \{\psi_j \cup \Psi_l \cup \Psi_r\}, \{\Theta_l \cup \Theta_r\}]$

Formally given array X and a 1-of-K encoding of the class labels $Y \in \mathbb{R}^{N\times 1} \rightarrow \mathcal{Y} \in \mathbb{I}^{N\times K}$, where $\mathcal{Y}_{nk} = 1$ indicates point n belongs to class k, we calculate

$$[\Phi, \cdot] = \text{CCA}\left(X, \mathcal{Y}\right) \tag{5}$$

where Φ are the canonical coefficients corresponding to X. For node j, the split projection vector ϕ_j is taken as the column of Φ for which the best split occurred during training and s_j as the corresponding best split point in $X\phi_j$. Finding the best such pair corresponds to function FINDBESTSPLIT$(\cdot)$ in Algorithm 2, which returns the index of the projection giving the best split ξ, the corresponding split point s_j and the respective value of split criterion relative to if the node were a leaf, denoted gain. Note that the CCA is only required during the training phase with the splitting rule (1) used directly for out of sample prediction.

Although the CCF training algorithm still uses feature subspacing (sampling λ features) in the same way as RF, it does

not use bagging[2]. Instead we introduce the projection bootstrap which calculates Φ using a local bootstrap sample of the data points $\{X', \mathcal{Y}'\}$, but then searches over possible splits in the projected space $X\Phi$ using the original dataset $\{X, \mathcal{Y}\}$ such that no information is discarded in the choice of $\{\phi_j, s_j\}$ given Φ.

Prior to running the CCA, the bootstrap sample is tested to ensure it contains more than one class and more than two unique data points. If there is only a single class or one unique point, one can either assign the node to be a leaf or replace the bootstrap sample with the original data when this does not have the same degeneracy. We found that either can be preferable depending on the dataset but take the latter as the default behaviour because this performed better on average in preliminary tests. If there are two unique points, the discriminant projection is set to be the vector between the two points, as shown in line 18 of Algorithm 2, instead of carrying out a CCA. The process of assigning a label to leaf, i.e. the $\text{LABEL}(\mathcal{Y})$ function in Algorithm 2, is simply the most populous class at the label. In the event of a tie, the function assigns the most populous of the tied classes at the parent node, recursing up the tree if required.

2.4 Data Preprocessing

The format of our forest definition given in Section 2.1 requires the data to be in numerical form. Ordered categorical features can be treated as numerical using the class index. For unordered categorical features $x^c \in \mathcal{S}$, where $\mathcal{S}$ represents the space of arbitrary qualitative attributes, we use a 1-of-K encoding. To ensure equal probability of selecting categorical and numerical features, the expanded binary array of each categorical feature is still treated as a single feature during feature subspacing. We refer to numeric, binary and ordered categorical features as ordinal and no-ordered categorical features as non-ordinal.

As described in lines 3-5 of Algorithm 1, we convert data points to their corresponding z-scores as a preprocessing step. Although this will not directly change the canonical correlation components, it does affect the rank reduction used in ensuring the numerical stability of CCA discussed in Section 2.5. Missing data is dealt with by setting its value to the training data mean.

2.5 Numerically Stable CCA

The closed form solution for CCA based on eigenvectors given in (4), can be numerically unstable if carried out naïvely, as it requires an inversion of the potentially degenerate covariance matrices. For example, if there are more features than data points, the covariance matrix is certain to be degenerate. Given the sequential partitioning of data in a decision tree, such degeneracy will become common as the tree depth increases, even if the covariances for the complete dataset are not degenerate. However, Björck and Golub [19] demonstrated that the solution for CCA can also be found in a numerically stable way. After centring both inputs, a QR decomposition with pivoting is carried out on each: $QR = WP$ for cantered input W, where Q is a unitary matrix, R is an upper triangular matrix and P is a pivot matrix such that the diagonal elements of R are of decreasing magnitude. If

$$\zeta = \max\left\{i : \left|R_{(i,i)}\right| > \varepsilon \left|R_{(1,1)}\right|\right\} \tag{6}$$

is the number of non-zero main diagonal terms within some tolerance ε, then the first ζ columns of Q will describe an orthonormal basis for the span of W. Therefore by applying the reductions $Q' \leftarrow Q_{(:,1:\zeta)}$ and $R' \leftarrow R_{(1:\zeta,1:\zeta)}$, then $Q'R'$ will be a pivoted reduction of W that is full rank and R' will be invertible. The algorithm then proceeds with the reduced matrices Q' and R' to carry out the CCA in a numerical stable manner, full details are provided in Appendix A.

Although for analytical application then the rank tolerance parameter ε should be taken as 0^+, we recommend taking a finite value (we use $\varepsilon = 10^{-4}$) to guard against numerical error and because this can act as a regularization term against individual splits overfitting the inputs. Note that packaged applications of this algorithm are available, for example CANONCORR in MATLAB, but in general these do not allow ε to be set manually.

3 Experiments

3.1 Comparison to State-of-the-art Tree Ensembles

To investigate the predictive performance of CCFs, we ran comparison tests against the state-of-the-art algorithms random forest (RF) and rotation forest over a broad variety of datasets. The results show that CCFs significantly outperformed both methods, creating a new benchmark in classification accuracy for out-of-the-box decision tree ensembles, despite being a considerably more computationally efficient than rotation forests as discussed in Section 4.3. In addition to comparing to these state-of-the-art methods, we also compared to a reduced version of our algorithm where we use tree bagging, as per RF, as an alternative to the projection bootstrap. We refer to this method as CCF-Bag.

For each method the ensemble was composed of $L = 500$ trees, noting that as forests converge with increasing L [1], the selection of L need only be based on computational budget. Each tree used the information gain split criterion of C4.5 [6] as the basis for choosing the best split, as is the default for WEKA's [20] implementations of RF and rotation forest. The choice of the information split criterion over the Gini criterion (the split criterion in MATLABs TREEBAGGER function and Breiman's original [1] implementation), was based on this giving better results for RF on the tested datasets. The RF, CCF-Bag and CCF algorithms were all implemented in MATLAB and we set the parameter for the number of features to sample at each step to $\lambda = \text{CEIL}(\log_2(D)+1)$ (where $D = D^r + D^c$ is the total number of features prior to the binary expansion of categorical features), with the exception that we set $\lambda = 2$ when $D = 3$ so that random subspacing and CCA can both be employed.

Rotation Forests were implemented in WEKA with 500 trees and the default options except that we used binary, unpruned, trees and set the minimum number of instances per leaf to 1. In addition to keeping the implementation of rotation forest as consistent as possible with the other algorithms, these settings dominated rotation forests of the same size with the default options over a single cross validation. As recommended by Rodriguez et al [16], 1-of-K encoding was used for non-ordinal features for rotation forests (note rotation forests do not then treat them differently to ordinal variables).

For each dataset, 15 different 10-fold cross-validation tests were performed. The majority of the 37 datasets were taken from the UCI machine learning database [21] with the exceptions of the *ORL* face recognition dataset [22], the *Polyadenylation Signal Prediction* (*polya*) dataset [23] and the artificial spiral dataset from

2. An exception to this is that bagging is used instead of the projection bootstrap when the number of features to be sampled, λ, is equal to the total number of present features. This is done to avoid overfitting.

TABLE 1: Dataset summaries and mean and standard deviations of percentage of test cases misclassified. Method with best accuracy is shown in bold. • and ○ indicate that CCFs were significantly better and worse respectively at the 1% level of a Wilcoxon signed rank test. K = number of classes, N = number of data points, D^c = number of non-ordinal features and D^r = number of ordinal features. The *ORL* and *Polya* datasets could not be run in reasonable time for rotation forest.

Data set	K	N	D^c	D^r	CCF	RF		Rotation Forest		CCF-Bag	
Balance scale	3	625	0	4	8.84 ± 3.73	18.66 ± 4.56	•	**7.25 ± 3.38**	○	8.84 ± 3.73	
Banknote	2	1372	0	4	**0.00 ± 0.00**	0.58 ± 0.64	•	**0.00 ± 0.00**		**0.00 ± 0.00**	
Breast tissue	6	106	0	9	27.64 ± 12.10	31.09 ± 12.38	•	28.48 ± 12.36		**27.33 ± 11.85**	
Climate crashes	2	360	0	18	6.33 ± 4.12	6.46 ± 4.10		**6.11 ± 3.94**	○	6.85 ± 4.10	•
Fertility	2	100	0	9	12.73 ± 9.40	14.53 ± 9.45	•	**12.40 ± 8.87**		12.73 ± 9.11	
Heart-SPECT	2	267	0	22	**17.16 ± 7.06**	18.86 ± 7.25	•	17.56 ± 7.29		18.25 ± 6.96	•
Heart-SPECTF	2	267	0	44	18.79 ± 7.09	18.91 ± 7.09		18.57 ± 7.06		**18.35 ± 6.87**	
Hill valley	2	1212	0	100	**0.00 ± 0.00**	39.16 ± 4.05	•	6.32 ± 2.65	•	**0.00 ± 0.00**	
Hill valley noisy	2	1212	0	100	**4.86 ± 1.84**	42.08 ± 4.57	•	11.01 ± 2.80	•	5.45 ± 2.02	•
ILPD	2	640	0	10	**28.05 ± 5.14**	29.92 ± 5.17	•	29.02 ± 5.25	•	28.32 ± 5.15	
Ionosphere	2	351	0	33	**4.78 ± 3.59**	6.53 ± 3.95	•	5.79 ± 3.56	•	5.30 ± 3.60	•
Iris	3	150	0	4	2.40 ± 3.73	5.07 ± 5.22	•	4.31 ± 5.19	•	**2.13 ± 3.73**	
Landsat satellite	2	6435	0	36	8.16 ± 1.02	8.03 ± 1.00	○	**7.75 ± 1.02**	○	8.57 ± 1.03	•
Letter	26	20000	0	16	**2.17 ± 0.33**	3.36 ± 0.39	•	2.43 ± 0.32	•	2.47 ± 0.38	•
Libras	15	360	0	90	10.37 ± 5.05	18.54 ± 5.93	•	**9.48 ± 4.47**	○	11.44 ± 5.20	•
MAGIC	2	19020	0	10	**11.59 ± 0.69**	11.90 ± 0.72	•	12.67 ± 0.71	•	11.69 ± 0.72	•
Nursery	5	12960	0	8	0.04 ± 0.06	0.19 ± 0.13	•	**0.03 ± 0.06**		0.08 ± 0.10	•
ORL	40	400	0	10304	1.85 ± 2.18	**1.72 ± 2.03**		-		2.00 ± 2.28	
Optical digits	10	5620	0	64	**1.27 ± 0.41**	1.59 ± 0.49	•	1.29 ± 0.41		1.46 ± 0.46	•
Parkinsons	2	195	0	22	**6.20 ± 5.20**	9.43 ± 6.17	•	7.19 ± 5.33	•	7.83 ± 6.14	•
Pen digits	10	10992	0	16	**0.41 ± 0.19**	0.82 ± 0.28	•	0.48 ± 0.22	•	0.45 ± 0.20	•
Polya	2	9255	0	169	**21.03 ± 1.26**	21.20 ± 1.27	•	-		21.22 ± 1.26	•
Seeds	3	210	0	7	4.95 ± 4.71	5.78 ± 5.01	•	**4.79 ± 4.60**		5.56 ± 4.89	•
Skin seg	2	245057	0	3	**0.03 ± 0.01**	0.05 ± 0.01	•	0.04 ± 0.01	•	0.03 ± 0.01	•
Soybean	19	683	13	22	**5.31 ± 2.82**	5.50 ± 3.02		5.67 ± 2.91		5.73 ± 3.11	•
Spirals	3	10000	0	2	**0.27 ± 0.15**	1.21 ± 0.33	•	1.01 ± 0.32	•	**0.27 ± 0.15**	
Splice	3	3190	60	0	**3.03 ± 0.89**	3.05 ± 0.93		4.21 ± 1.16	•	3.08 ± 0.91	
Vehicle	4	846	0	18	**18.20 ± 4.13**	25.22 ± 4.57	•	21.12 ± 4.27	•	18.38 ± 4.19	
Vowel-c	11	990	2	10	**0.90 ± 0.93**	2.56 ± 1.66	•	0.95 ± 0.94		1.26 ± 1.12	•
Vowel-n	11	990	0	10	1.72 ± 1.30	3.93 ± 1.98	•	**1.43 ± 1.19**	○	2.38 ± 1.43	•
Waveform (1)	3	5000	0	21	13.54 ± 1.56	15.06 ± 1.69	•	13.53 ± 1.50		**13.39 ± 1.52**	○
Waveform (2)	3	5000	0	40	13.39 ± 1.68	14.61 ± 1.64	•	13.31 ± 1.64		**13.28 ± 1.58**	
Wholesale-c	2	440	1	7	8.50 ± 4.13	**8.15 ± 4.01**		8.44 ± 3.99		8.42 ± 3.96	
Wholesale-r	3	440	0	7	29.80 ± 5.93	28.97 ± 6.10	○	**28.18 ± 6.19**	○	28.39 ± 6.15	○
Wisconsin cancer	2	699	0	9	3.10 ± 1.95	3.54 ± 2.17	•	**2.87 ± 1.82**		3.04 ± 1.95	
Yeast	10	1484	0	8	38.02 ± 3.98	37.89 ± 4.22		37.21 ± 4.23	○	**37.12 ± 4.05**	○
Zoo	7	101	0	16	**3.20 ± 5.71**	5.13 ± 6.73	•	5.47 ± 6.71	•	3.47 ± 5.79	

TABLE 2: Number of victories column vs row at 1% significance level of Wilcoxon signed rank test

	CCF	RF	Rotation Forest	CCF-Bag
CCF	-	2	7	3
RF	**28**	-	28	28
Rotation Forest	**14**	2	-	12
CCF-Bag	**18**	2	10	-

figure 1. Summaries of the datasets along with the results are given in Table 1. Note for the *vowel-c* dataset the sex and identifier for the speaker are included whereas these are omitted for the *vowel-n* dataset which is otherwise identical. The *wholesale-c* and *wholesale-r* datasets correspond to predicting the *channel* and *region* attributes respectively.

Table 2 shows a summary of results over all the datasets, giving the number of datasets for which the performance of one dataset was significantly better than another at the 1% level of a Wilcoxon signed rank test. This shows that CCFs performed excellently. The improvement over RF was particularly large, with RF having on average 1.77 times as many misclassifications as CCF (ignoring the two datasets where CCF had perfect accuracy). To give another perspective, if one were using RF and decided to switch to CCF, then the number of misclassifications would be reduced by a factor of 29.0% on average for the tested datasets. The domination of CCFs over CCF-Bag highlights the improvement from the projection bootstrap, while the good performance on a large variety of datasets demonstrates the robustness and wide ranging applicability of CCFs.

3.2 Comparison to Other Classifiers

In order to provide comparison to a wider array of classifiers, we also tested CCFs using the experiments of Fernández-Delgado et al [4] from their recent survey of 179 classifiers applied to 121 datasets. We used the same partitions which were a mix of 4-fold cross validations and predefined train / test splits[3]. We omitted datasets containing non-ordinal features on the basis that they pre-processed such features by treating the category indexes as numeric features, instead of our recommended procedure (see section 2.4). The *image-segmentation* dataset was also omitted as we were unable to replicate the RF results of the original test. In

3. Partitions and results from [4] are available at http://persoal.citius.usc.es/manuel.fernandez.delgado/papers/jmlr/

TABLE 3: Comparison of top 20 performing classifiers on 82 UCI datasets. R is the mean rank over all 180 classifiers according to error rate; E is the mean error rate (%); κ is the mean Cohen's κ [24]; E_{CCF} and κ_{CCF} are the respective values for CCFs on the datasets where the competing classifier successfully ran (note CCFs successfully ran on all datasets); N_v and N_l are the number of datasets where the CCFs κ was higher and lower than the classifier respectively; and p is the p-value for whether the CCFs κ mean is higher using a Wilcoxon signed ranks test. Classifier types: SVM = support vector machine, NNET = neural net, RF = random forest, Bag = bagging and BST = boosting. For details on classifiers see [4].

Classifier	R	E	E_{CCF}	κ	κ_{CCF}	N_v	N_l	p
CCF	**28.87**	**14.08**	-	**70.67**	-	-	-	-
svmPoly (SVM)	31.53	15.73	14.27	65.10	69.61	54	25	2.3e-4
svmRadialCost (SVM)	31.84	15.33	14.27	66.55	69.61	43	36	0.11
svm_C (SVM)	32	15.67	14.18	67.65	70.49	46	32	0.18
elm_kernel (NNET)	32.19	15.20	14.54	69.01	69.75	42	36	0.16
parRF (RF)	33.03	15.54	14.08	67.73	70.67	52	27	0.014
svmRadial (SVM)	33.77	15.68	14.27	65.88	69.61	50	28	1.6e-3
rf_caret (RF)	34.48	15.56	14.18	67.67	70.49	54	23	6.3e-4
rforest_R (RF)	40.70	15.82	14.18	66.67	70.49	57	20	2e-5
TreeBagger (RF)	40.91	15.75	14.08	67.51	70.67	55	23	3.5e-5
Bag_LibSVM (Bag)	42.28	16.65	14.25	58.13	70.27	70	12	3.2e-12
C50_t (BST)	42.61	16.85	14.08	66.11	70.67	57	22	4.0e-4
nnet_t (NNET)	42.87	18.74	14.08	64.72	70.67	54	26	1.5e-3
avNNet_t (NNET)	43.26	18.77	14.08	64.88	70.67	50	29	1.0e-3
RotationForest	44.62	16.64	14.08	65.34	70.67	64	15	7.1e-9
pcaNNet_t (NNET)	45.86	19.28	14.08	63.83	70.67	54	25	1.5e-4
mlp_t (NNET)	46.06	17.38	14.08	66.75	70.67	54	26	1.6e-3
LibSVM (SVM)	46.50	16.65	14.08	63.80	70.67	57	21	2.9e-6
MB_LibSVM (BST)	46.90	16.82	14.25	64.47	70.27	61	17	1.8e-6
RRF_t (RF)	49.56	16.71	14.18	66.30	70.49	59	20	1.1e-5

total 82 datasets were compared, for which summaries along with detailed results are available in Appendix C.

Whereas [4] included an, often intensive, parameter tuning step in their tests, we used CCFs in an out-of-the-box fashion, taking the same parameters as in Section 3.1. As a check that tests were run correctly, we also ran MATLAB's TREEBAGGER algorithm, with 500 trees and $\lambda = \text{CEIL}(\log_2(D) + 1)$, which as expected gave performance on par with the very similar rforest_R algorithm. A summary of the results for the top 20 performing classifiers (based on average accuracy rank) is given in table 3. Despite using no parameter tuning, CCFs outperformed all other tested classifiers based on every calculated performance metric.

4 DISCUSSION

4.1 Relationship with Linear Discriminant Analysis

As shown by, for example, De la Torre [25], CCA with 1-of-K class encoding is exactly equivalent to Rao's [26] extension of FLDA to the multi-class case. We have presented our work as the former because we believe that considering uncorrelated sets of co-projections which maximise correlation between features and classes labels is an intuitive way to understand the multiple solutions from a multi-class FLDA and because of the relative ease of carrying out CCA in a numerically stable fashion.

4.2 Effect of Correlation

As shown by Menze et al [15], RFs often struggle on data with highly correlated features. CCA naturally incorporates information about feature correlations, therefore CCFs do not suffer the same issues. This is demonstrated by their superior performance on the highly correlated *hill valley* datasets.

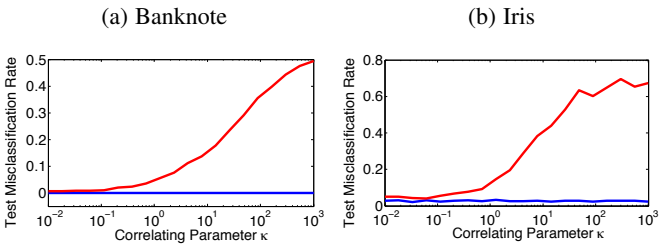

Fig. 2: Misclassification rate of CCFs (blue) and RFs (red) on artificially correlated data. For each method, 5 separate 10-fold cross validations were run and the mean test accuracy across the 50 tests reported. ε was set to 10^{-12} to prevent the variation corresponding to the original data being eliminated in the rank reduction step of the CCA calculation for large κ.

To further investigate the effect of correlation, we used the following method of artificially correlating the data (after carrying out the preprocessing described in section 2.4):

1) Add a new random feature $X_{(D+1,n)} \sim \mathcal{N}(0, \kappa)$, $\forall n = 1, \ldots, N$ where κ is a parameter which will control the degree of correlation to be added.
2) To each of the existing features, randomly either add or subtract the new feature:
$$X_{(:,d)} \leftarrow X_{(:,d)} + \zeta_d X_{(:,D+1)}, \ \forall d = 1, \ldots, D$$
where $\zeta_d \overset{\text{i.i.d}}{\sim} \text{UNIFORM-DISCRETE}\{-1, 1\}$.

As shown in figure 2, this transformation has no effect on the accuracy of CCFs, whereas the accuracy of RF decreases with increasing κ, eventually giving the same accuracy as random prediction. The use of PCA means rotation forests exhibit similar robustness to global correlations as CCFs.

We postulate that CCFs are better than rotation forests at incorporating class dependent and localized correlations. This is because the rotation step of rotation forests does not incorporate any class information other than in the random elimination of classes. Further, individual trees in a rotation forest are orthogonal and therefore cannot incorporate spatial variation in correlation. The self similar nature of the growth algorithm for CCTs, on the other hand, means that the local correlations of a partition can be incorporated as naturally as the global correlations.

To investigate these suggestions formally, we tested performance on compound datasets in which localized and class dependent correlations had been artificially added. A replica of the dataset with the classes in the replica treated separately was created, such that if a point has class k in the original dataset, it has class $k + K$ in the replica. The features in the original and the replica were independently correlated and a constant added to replica to separate it from the original. Formally:

$$X \leftarrow \begin{bmatrix} \text{CORR}(X) \\ \text{CORR}(X) + \beta \mathbb{1}^{N \times (D+1)} \end{bmatrix}, \quad \mathcal{Y} \leftarrow \begin{bmatrix} \mathcal{Y} & \mathbf{0} \\ \mathbf{0} & \mathcal{Y} \end{bmatrix} \tag{7}$$

where CORR denotes the correlation process described earlier in the section and β is a scalar dictating the degree of separation.

We performed a single crossfold validation on a selection of the datasets from table 1, taking $\beta = 2000$ and $\kappa = 100$. The results, given in Table 4, show that CCFs only experienced a small

TABLE 4: Mean and standard deviations of percentage of test cases misclassified for compound datasets. Method with best accuracy is shown in bold. • and ○ indicate that CCFs were significantly better and worse respectively at the 5% level of a Wilcoxon signed rank test.

Data set	CCF	RF		Rotation Forest	
Balance Scale	**7.84 ± 2.08**	47.12 ± 3.76	•	20.24 ± 4.46	•
Banknote	**0.00 ± 0.00**	35.29 ± 2.76	•	2.85 ± 0.62	•
Iris	**3.67 ± 2.77**	70.33 ± 7.52	•	19.67 ± 9.87	•
Landsat satellite	**8.64 ± 0.88**	32.64 ± 1.14	•	11.56 ± 0.82	•
Libras	11.53 ± 2.85	89.58 ± 4.57	•	**7.36 ± 2.45**	○
Parkinsons	**8.97 ± 3.67**	32.82 ± 7.93	•	12.56 ± 6.22	•
Vowel-n	**3.13 ± 0.71**	86.06 ± 2.04	•	20.20 ± 2.79	•
Wholesale-r	31.02 ± 3.03	37.39 ± 5.68	•	**28.18 ± 4.82**	
Wisconsin cancer	**2.86 ± 1.56**	30.64 ± 2.94	•	2.93 ± 1.66	
Yeast	**38.86 ± 1.85**	70.17 ± 3.20	•	56.09 ± 1.85	•

loss of accuracy on all of the datasets, whereas there was a large loss of accuracy in all cases for RFs and on some of the datasets for rotation forests. This supports our hypothesis that CCFs are better than rotation forests at dealing with localized correlations.

4.3 Computational Complexity

For L trees, N data points, K classes and λ features used at each node, the average case training computational complexity of RF is $\mathrm{O}\left(NL\lambda\left(\log N\right)^2\right)$ [27]. The two limiting factors for the complexity of CCFs are the search over possible splits and the CCA calculations. Assuming all features are ordinal, the search over splits for CCFs has the same complexity as RF except that one must search over $\nu = \min\left(\lambda, K-1\right)$ dimensions at each node. The theoretically achievable[4] combined complexity for all CCA calculations across the forest is $\mathrm{O}\left(NL\lambda^2 \log N\right)$, giving a total complexity of $\mathrm{O}\left(NL\nu\left(\log N\right)^2 + NL\lambda^2 \log N\right)$. The first of these terms is upper bounded by the complexity of RF, while the second term also is if $\lambda < \log N$. Using the recommended value of $\lambda = \textsc{ceil}(\log_2\left(D\right)+1)$ this means the complexity of CCF is upper bounded by that of RF whenever $N > D$ and may be noticeably lower if N is large and K is small. In practise the constant factor for the CCA is typically less than the split search and empirically we found that even for the ORL dataset ($N = 400,\ D = 10304,\ K = 40$) with the default of $\lambda = 15$, only around $1/6$ of the time was taken in the CCA calculations.

Should one wish to use λ significantly larger than the suggested default, speeds gains would be achievable by separately generate M projection matrices $\{\Phi_m\}_{m=1:M}$, each using λ/M features, and search for the optimal split over all generated projections. Note if $M = \lambda$, Breiman's RF algorithm is recovered.

In the presence of non-ordinal features, λ is replaced with the number of features used after the 1-of-K encoding is applied in the CCF complexity. Therefore if the data contains non-ordinal features with a large number of possible values, it may be computationally preferable to consider the 1-of-K expanded features as separate entities during feature subspacing.

4. The numerically stable method used for experiments and outlined in Appendix A is actually $\mathrm{O}\left(NL\left(\lambda^2+K^2\right)\log N\right)$, with the additional term occuring due to the QR decomposition of the centred $\mathcal{Y}$. In practise we found the constant factor for this term to be very small and therefore that this was not a problem. However, for datasets with a very large K, an alternative method for CCA might be preferable, for example by exploiting the LDA equivalence, if numerical stability can be ensured by other means.

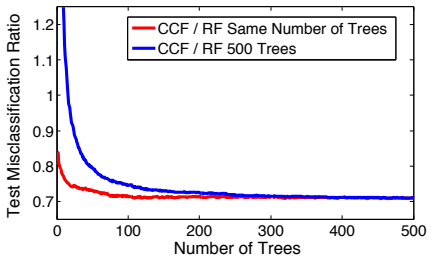

Fig. 3: Mean misclassification ratios for 37 datasets in Table 1. The red line shows the average across the datasets of the ratio between the number of CCF and RF test misclassifications for forests of the same size. The blue line gives the same ratio when comparing CCFs of varying number of trees to a RF with 500 trees.

Rotation forest training requires each tree to search the full set of features and therefore has a training complexity of $\mathrm{O}\left(NLD\left(\log N\right)^2\right)$. This is exponentially more expensive in the number of features than RFs and CCFs when λ is set to a logarithmic factor of D. This makes their implementation impractical for datasets with more than a modest number of features, as demonstrated by the *ORL* and *polya* datasets for which we were unable to train a rotation forest, experiencing both memory issues and an impractically long training time.

4.4 Effect of Number of Trees

To investigate the variation in performance with the number of trees we used the individual tree predictions from 3.1 to evaluate the accuracy of RF and CCF for different ensemble sizes. Figure 3 summarises the results and shows that, as expected, it is always beneficial to use more trees, but that there are diminishing returns. Some datasets require more trees than others before the accuracy begins to saturate (not shown), but the advantages of CCFs over RFs is maintained across all ensemble sizes (though for a very small number of trees this is slightly less pronounced). A further results of interest is that on average it only takes around 15 CCF trees to match the accuracy of 500 RF trees. One could therefore envisage using a smaller CCF as a fast and accurate alternative to a larger RF under a restricted computational budget.

4.5 Related Work

Since our development of CCFs, we became aware of recent similar work by Zhang and Suganthan [28]. In addition to the large improvements we have shown by using projection bootstrapping instead of bagging, we believe our method has two significant advantages over their method. Firstly their method of dealing with categorical features by carrying out LDA on all possible permutations can lead to combinatorial computational complexity and will therefore be intractable when the number of categorical features is large. Secondly, their method of carrying out LDA by finding the generalized eigenvectors of the between-class and within-class scatter matrices can easily become numerically unstable.

As Zhang and Suganthan performed the same cross validation tests on 14 of the common datasets, it is possible to make numerical comparisons. Taking the first 100 trees from our experiments to match the ensemble sizes and using a t-test at the 1% significance level, gives win/draw/loss ratios for CCFs of 9/5/0 and 10/4/0

compared to PCA-RF and LDA-RF respectively. On average PCA-RF and LDA-RF had 1.70 and 1.53 times as many misclassifications as CCFs respectively. These results demonstrate that CCFs give a significant improvement in empirical performance over both PCA-RF and LDA-RF.

Donoser and Schmalstieg [29] recently developed a method in which they use CCA as a preliminary step in a random fern classifier [30]. Their method shares many similarities with rotation forests with each fern trained using a separate global CCA projection. Although their method offers the potential for computational gains for large datasets, it is only suitable when there are a large number of classes. Further, the lack of hierarchical splits restricts the ability to learn local structure, with ferns typically giving lower predictive accuracy that tree ensemble methods.

5 Conclusions and Future Work

We have introduced canonical correlation forests, a new decision tree ensemble learning scheme that creates a new performance benchmark for out-of-box tree ensemble classifiers and potentially black-box classification in general, despite being significantly less computationally expensive than some of the previously best alternatives. This performance is based on two core innovations: the use of a numerically stable CCA for generating projections along which the trees split and a novel new alternative to bagging, the projection bootstrap, which retains the full dataset for split selection in the projected space.

As it is the aim of the CCF method to operate in a parameter free context, we have made no attempt to adjust any algorithm operation between datasets and have made little investigation as to whether our choices of default parametrisation are in fact the best. The method is fully compatible with alternative meta schemes such as boosting or training each tree on a rotated coordinate system, such as done for rotation forests. Zhang and Suganthan's [28] RF-ensemble extension could also easily be applied to CCFs and might offer further improvement. Weighted voting schemes for trees such as Bayesian model combination [31] and similarity based schemes [32] would directly apply to CCFs and may also offer improvement at the cost of additional complexity, computational time and in some cases the need for additional parameter adjustment. All the concepts introduced should also directly apply to random forest regression models, providing a natural extension.

Acknowledgments

Tom Rainforth is supported by a BP industrial grant.

References

[1] L. Breiman, "Random forests," *Machine learning*, vol. 45, no. 1, pp. 5–32, 2001.
[2] P. Geurts, D. Ernst, and L. Wehenkel, "Extremely randomized trees," *Machine learning*, vol. 63, no. 1, pp. 3–42, 2006.
[3] J. H. Friedman, "Greedy function approximation: a gradient boosting machine," *Annals of statistics*, pp. 1189–1232, 2001.
[4] M. Fernández-Delgado, E. Cernadas, S. Barro, and D. Amorim, "Do we need hundreds of classifiers to solve real world classification problems?" *The Journal of Machine Learning Research*, vol. 15, no. 1, pp. 3133–3181, 2014.
[5] L. Breiman, J. Friedman, C. J. Stone, and R. A. Olshen, *Classification and regression trees*. CRC press, 1984.
[6] J. R. Quinlan, *C4. 5: programs for machine learning*. Elsevier, 2014.
[7] T. K. Ho, "Random decision forests," in *Document Analysis and Recognition, 1995., Proceedings of the Third International Conference on*, vol. 1. IEEE, 1995, pp. 278–282.
[8] ——, "The random subspace method for constructing decision forests," vol. 20, pp. 832–844, 1998.
[9] L. Breiman, "Bagging predictors," *Machine learning*, vol. 24, no. 2, pp. 123–140, 1996.
[10] S. K. Murthy, S. Kasif, and S. Salzberg, "A system for induction of oblique decision trees," *arXiv preprint cs/9408103*, 1994.
[11] J. Gama, "Functional trees," *Machine Learning*, vol. 55, no. 3, pp. 219–250, 2004.
[12] W.-Y. Loh and Y.-S. Shih, "Split selection methods for classification trees," *Statistica sinica*, vol. 7, no. 4, pp. 815–840, 1997.
[13] R. A. Fisher, "The use of multiple measurements in taxonomic problems," *Annals of eugenics*, vol. 7, no. 2, pp. 179–188, 1936.
[14] T. D. Lemmond, A. O. Hatch, B. Y. Chen, D. Knapp, L. Hiller, M. Mugge, and W. G. Hanley, "Discriminant random forests." in *DMIN*, 2008, pp. 55–61.
[15] B. H. Menze, B. M. Kelm, D. N. Splitthoff, U. Koethe, and F. A. Hamprecht, "On oblique random forests," in *Machine Learning and Knowledge Discovery in Databases*. Springer, 2011, pp. 453–469.
[16] J. J. Rodriguez, L. I. Kuncheva, and C. J. Alonso, "Rotation forest: A new classifier ensemble method," *Pattern Analysis and Machine Intelligence, IEEE Transactions on*, vol. 28, no. 10, pp. 1619–1630, 2006.
[17] H. Hotelling, "Relations between two sets of variates," *Biometrika*, pp. 321–377, 1936.
[18] M. Borga, "Canonical correlation: a tutorial," *On line tutorial http://people.imt.liu.se/magnus/cca*, vol. 4, 2001.
[19] A. Björck and G. H. Golub, "Numerical methods for computing angles between linear subspaces," *Mathematics of computation*, vol. 27, no. 123, pp. 579–594, 1973.
[20] M. Hall, E. Frank, G. Holmes, B. Pfahringer, P. Reutemann, and I. H. Witten, "The weka data mining software: an update," *ACM SIGKDD explorations newsletter*, vol. 11, no. 1, pp. 10–18, 2009.
[21] M. Lichman, "Uci machine learning repository," 2013.
[22] F. S. Samaria and A. C. Harter, "Parameterisation of a stochastic model for human face identification," in *Applications of Computer Vision, 1994., Proceedings of the Second IEEE Workshop on*, 1994, pp. 138–142.
[23] J. Li and H. Liu, "Kent ridge bio-medical data set repository," *Institute for Infocomm Research. http://sdmc.lit.org.sg/GEDatasets/Datasets*, 2002.
[24] J. Carletta, "Assessing agreement on classification tasks: the kappa statistic," *Computational linguistics*, vol. 22, no. 2, pp. 249–254, 1996.
[25] F. De la Torre, "A least-squares framework for component analysis," *Pattern Analysis and Machine Intelligence, IEEE Transactions on*, vol. 34, no. 6, pp. 1041–1055, 2012.
[26] C. R. Rao, "The utilization of multiple measurements in problems of biological classification," *Journal of the Royal Statistical Society. Series B (Methodological)*, vol. 10, no. 2, pp. 159–203, 1948.
[27] G. Louppe, "Understanding random forests: From theory to practice," *arXiv preprint arXiv:1407.7502*, 2014.
[28] L. Zhang and P. N. Suganthan, "Random forests with ensemble of feature spaces," *Pattern Recognition*, vol. 47, no. 10, pp. 3429–3437, 2014.
[29] M. Donoser and D. Schmalstieg, "Discriminative feature-to-point matching in image-based localization," in *Computer Vision and Pattern Recognition (CVPR), 2014 IEEE Conference on*. IEEE, 2014, pp. 516–523.
[30] M. Özuysal, M. Calonder, V. Lepetit, and P. Fua, "Fast keypoint recognition using random ferns," *Pattern Analysis and Machine Intelligence, IEEE Transactions on*, vol. 32, no. 3, pp. 448–461, 2010.
[31] K. Monteith, J. L. Carroll, K. Seppi, and T. Martinez, "Turning bayesian model averaging into bayesian model combination," in *Neural Networks (IJCNN), The 2011 International Joint Conference on*. IEEE, 2011.
[32] M. Robnik-Šikonja, "Improving random forests," in *Machine Learning: ECML 2004*. Springer, 2004, pp. 359–370.

APPENDIX A NUMERICALLY STABLE CCA SOLUTION IN DETAIL

Algorithm 3 outlines the numerically stable method used to carry out CCA. Here $[q, r, p] = \mathrm{QR}(\alpha)$ refers to a QR decomposition with pivoting such that $qr = \alpha_{(:,p)}$ where q is an orthogonal matrix, r is upper triangular matrix and p is a column ordering defined implicitly such that $|r(i,i)| > |r(j,j)| \ \forall i < j$. Here $[u, \Omega, z] = \mathrm{SVD}(\alpha)$ refers to a singular value decomposition such that $u\Omega z^T = \alpha$ where u and z are unitary matrix and Ω is diagonal matrix of singular values, with the ordering defined such that $\Omega(i,i) > \Omega(j,j) \ \forall i < j$.

The core idea of the algorithm is that reducing q^w, q^v, r^w and r^v such that r^w and r^v are full rank, ensures that r^w and r^v are invertible. Further as the r matrices are upper triangular, the coefficient calculation of line 18 can be simply calculated by back substitution without the need for inversion.

Algorithm 3: Numerically Stable CCA

Inputs: First array $w \in \mathbb{R}^{N \times D}$, second array $v \in \mathbb{R}^{N \times K}$, tolerance parameter $\varepsilon \in [0^+, 1^-]$
Outputs: Projection matrices for first and second arrays A and B, correlations ρ

1: $\mu^w = \frac{1}{N} \sum_{n=1:N} w_{(n,:)}$ ▷ First centre the inputs
2: $\mu^v = \frac{1}{N} \sum_{n=1:N} v_{(n,:)}$
3: $w_{(:,d)} \leftarrow w_{(:,d)} - \mu^w_{(d)} \quad \forall d \in \{1, \ldots, D\}$
4: $v_{(:,k)} \leftarrow v_{(:,k)} - \mu^v_{(k)} \quad \forall k \in \{1, \ldots, K\}$
5: $[q^w, r^w, p^w] = \mathrm{QR}(w)$ ▷ Carry out pivoted QR decompositions
6: $[q^v, r^v, p^v] = \mathrm{QR}(v)$
7: $\zeta^w = \max\{i : |r^w_{(i,i)}| < \varepsilon |r^w_{(1,1)}|\}$
8: $\zeta^v = \max\{i : |r^v_{(i,i)}| < \varepsilon |r^v_{(1,1)}|\}$
9: $q^w \leftarrow q^w_{(:,1:\zeta^w)}, \quad r^w \leftarrow r^w_{(1:\zeta^w,1:\zeta^w)}$ ▷ Reduce to full rank
10: $q^v \leftarrow q^v_{(:,1:\zeta^v)}, \quad r^v \leftarrow r^v_{(1:\zeta^v,1:\zeta^v)}$
11: $\nu_{\max} = \min(\zeta^w, \zeta^v)$ ▷ Number of coefficient pairs that will be returned
12: **if** $\zeta^w > \zeta^v$ **then** ▷ Select which of two equivalent SVD decompositions is faster
13: $\quad [u, \Omega, z] = \mathrm{SVD}((q^w)^T q^v)$
14: **else**
15: $\quad [z, \Omega, u] = \mathrm{SVD}((q^v)^T q^w)$
16: **end if**
17: $u \leftarrow u_{(:,1:\nu_{\max})}, \quad z \leftarrow z_{(:,1:\nu_{\max})}$ ▷ Remove meaningless components
18: $A = (r^w)^{-1} u$ ▷ As r^w and r^v are upper triangular these can be solved by back substitution
19: $B = (r^v)^{-1} z$
20: $\rho = \mathrm{DIAG}(\Omega)$
21: $A_{(p^w,:)} \leftarrow \left[A^T, \mathbf{0}\right]^T$ ▷ Reorder rows to match corresponding columns in original matrices
22: $B_{(p^v,:)} \leftarrow \left[B^T, \mathbf{0}\right]^T$ ▷ Some rows are set to zero if original matrix was not full rank
23: **return** A, B, ρ

APPENDIX B INVERTED CROSS VALIDATION

To investigate the performance of CCFs on datasets containing few data points relative to the complexity of the underlying structure, we carried out inverted cross validations, training on one fold and testing on the other nine. 15 such tests were carried out, using the same folds as the original cross validation. Table 5 gives the results on each of the individual datasets and Table 6 gives a summary of the significant victories and losses. The parameters used were the same as for the standard cross validation except that only 200 trees were used for computational reasons.

The performance of CCFs relative to rotation forests was similar to the standard cross validation case. CCF-Bag performed relatively more favourably compared with CCFs , but was still comprehensively outperformed. The relative performance of RFs to the other methods improved slightly but it was still the worst performing method by a large margin.

All methods performed worse than predicting the most popular class for the *fertility* and *wholesale-r* datasets, which gives misclassification rates of 12.0% and 28.2% respectively. This suggests that it may be beneficial to incorporate information about the overall class ratios into the algorithm in some way.

TABLE 5: Mean and standard deviations of percentage of test cases misclassified for inverted cross validation. Method with best accuracy is shown in bold. • and ○ indicate that CCFs were significantly better and worse respectively at the 1% level of a Wilcoxon signed rank test.

Data set	CCF	RF		Rotation Forest		CCF-Bag	
Balance scale	14.86 ± 2.54	21.02 ± 2.74	•	15.27 ± 2.52	•	**14.08 ± 2.59**	○
Banknote	**0.64 ± 0.57**	3.96 ± 1.66	•	0.89 ± 0.70	•	0.78 ± 0.58	•
Breast tissue	**50.51 ± 8.19**	52.06 ± 7.72	•	51.03 ± 8.10		54.76 ± 8.87	•
Climate crashes	7.23 ± 0.65	**7.22 ± 0.51**		7.22 ± 0.79		7.22 ± 0.54	
Fertility	18.97 ± 8.16	**14.20 ± 5.36**	○	15.38 ± 5.92	○	16.76 ± 7.20	○
Heart-SPECT	20.63 ± 3.08	20.76 ± 3.06		20.09 ± 3.22	○	**20.04 ± 2.83**	○
Heart-SPECTF	21.11 ± 1.87	**20.79 ± 1.93**	○	20.93 ± 2.05	○	21.38 ± 2.56	
Hill valley	**0.14 ± 0.39**	48.34 ± 1.75	•	7.18 ± 1.77	•	0.17 ± 0.45	
Hill valley noisy	**20.37 ± 4.07**	49.27 ± 1.48	•	22.22 ± 3.50	•	21.63 ± 4.57	•
ILPD	30.65 ± 1.79	30.68 ± 1.71		**30.14 ± 1.52**	○	30.29 ± 1.62	○
Ionosphere	**11.90 ± 4.05**	13.90 ± 4.44	•	12.95 ± 4.28	•	16.78 ± 4.82	•
Iris	5.93 ± 3.83	7.59 ± 4.31	•	9.74 ± 5.64	•	**5.65 ± 4.13**	
Landsat satellite	11.58 ± 0.41	12.07 ± 0.49	•	**11.41 ± 0.45**	○	12.19 ± 0.42	•
Letter	**10.14 ± 0.47**	13.46 ± 0.57	•	11.14 ± 0.48	•	11.22 ± 0.48	•
Libras	**49.86 ± 4.83**	61.57 ± 4.31	•	55.27 ± 4.82	•	52.30 ± 4.66	•
MAGIC	**13.46 ± 0.22**	14.03 ± 0.28	•	14.19 ± 0.29	•	13.55 ± 0.23	•
Nursery	3.15 ± 0.34	3.97 ± 0.43	•	**2.89 ± 0.39**	○	3.67 ± 0.36	•
ORL	**54.95 ± 3.80**	60.35 ± 4.04	•	-		61.22 ± 3.74	•
Optical digits	**3.54 ± 0.38**	4.79 ± 0.47	•	3.91 ± 0.42	•	3.93 ± 0.38	•
Parkinsons	**17.06 ± 4.05**	18.75 ± 4.02	•	18.55 ± 4.43	•	18.24 ± 4.62	•
Pen digits	**1.43 ± 0.22**	2.97 ± 0.35	•	1.84 ± 0.27	•	1.67 ± 0.24	•
Polya	23.80 ± 0.51	24.16 ± 0.61	•	**23.08 ± 0.50**	○	23.84 ± 0.50	
Seeds	8.84 ± 3.14	13.34 ± 3.21	•	11.71 ± 3.70	•	**8.53 ± 3.21**	○
Skin seg	**0.06 ± 0.01**	0.13 ± 0.02	•	0.10 ± 0.01	•	**0.06 ± 0.01**	
Soybean	**18.96 ± 3.95**	21.99 ± 4.00	•	21.22 ± 4.73	•	20.23 ± 4.06	•
Spirals	**0.68 ± 0.16**	3.29 ± 0.49	•	3.80 ± 0.57	•	**0.68 ± 0.16**	
Splice	7.53 ± 1.75	**4.81 ± 0.68**	○	6.72 ± 1.11	○	9.06 ± 2.12	•
Vehicle	**26.02 ± 2.14**	32.76 ± 2.66	•	27.79 ± 2.31	•	26.78 ± 2.26	•
Vowel-c	**40.71 ± 3.17**	46.42 ± 3.00	•	41.63 ± 2.87	•	41.46 ± 3.44	•
Vowel-n	**34.15 ± 2.99**	41.52 ± 2.94	•	35.82 ± 3.16	•	35.37 ± 2.92	•
Waveform (1)	14.76 ± 0.41	16.52 ± 0.53	•	14.91 ± 0.42	•	**14.66 ± 0.41**	○
Waveform (2)	14.83 ± 0.48	16.24 ± 0.49	•	14.83 ± 0.49		**14.70 ± 0.47**	○
Wholesale-c	11.41 ± 2.14	10.82 ± 2.00	○	**10.58 ± 1.84**	○	11.16 ± 2.13	○
Wholesale-r	35.64 ± 4.09	33.38 ± 3.66	○	**31.23 ± 3.59**	○	33.08 ± 3.81	○
Wisconsin cancer	4.12 ± 1.02	4.31 ± 0.98	•	**3.53 ± 0.69**	○	4.10 ± 1.03	
Yeast	46.12 ± 1.86	45.98 ± 1.91		**45.32 ± 1.82**	○	45.37 ± 1.83	○
Zoo	**23.43 ± 10.80**	25.36 ± 11.26	•	24.10 ± 10.66		24.12 ± 11.15	•

TABLE 6: Number of victories column vs row at 1% significance level of Wilcoxon signed rank test for inverted cross fold validation

	CCF	RF	Rotation Forest	CCF-Bag
CCF	-	5	12	10
RF	**28**	-	26	26
Rotation Forest	**20**	5	-	15
CCF-Bag	**19**	8	12	-

APPENDIX C DETAILED RESULTS FOR COMPARISONS TO OTHER CLASSIFIERS

Table 7 gives a detailed comparison of CCFs to MATLAB's TREEBAGGER algorithm, along with a comparison to a summary of the performance of the 179 classifiers tested in [4] for 82 UCI datasets. Both CCFs and TREEBAGGER used 500 trees and $\lambda = \text{CEIL}(\log_2(D) + 1)$. For significance comparisons with the TREEBAGGER algorithm a 10% significance level was necessary as the Wilcoxon signed rank test cannot give a p-value lower than 6.25% for 4-fold cross validation. This gave a win/draw/loss ratio for CCFs of 22/56/4. It should be noted that the number of losses is no more than would be expected by chance and that the reason that there are many more draws than in the tests of Section 3.1 is that a many fewer tests were carried out for each dataset (4 instead of 150). There were a number of datasets were CCFs performed noticeably better then any of the other classifiers, with the performance on the *hill-valley-noisy* dataset particularly impressive, giving a error rate of 6.93% with the next best classifier only achieving 25.7%.

TABLE 7: Dataset summaries and mean and standard deviations of percentage of test cases misclassified for CCFs and TREEBAGGER on 82 datasets used for comparison to classifiers used in [4]. Datasets were a predefined train / test split was used instead of a 4-fold cross validation have no standard deviation given. K = number of classes, N = number of data points and D = number of features. Method with best accuracy is shown in bold. • and ○ indicate that CCFs were significantly better and worse respectively at the 10% level of a Wilcoxon signed rank test. Also shown is the average and standard deviation, best and worst for the error rate across the 178 classifiers (not including CCF and TREEBAGGER), and N_B and N_W the number of classifiers that were better and worse than CCFs respectively.

Data set	K	N	D	CCF	TREEBAGGER		Average	Best	Worst	N_B	N_W
abalone	3	4177	8	**34.15 ± 1.53**	35.42 ± 0.99	•	39.91 ± 7.52	32.6	65.4	14	157
acute-inflammation	2	120	6	**0.00 ± 0.00**	**0.00 ± 0.00**		5.14 ± 12.97	0.0	50.9	0	50
acute-nephritis	2	120	6	**0.00 ± 0.00**	**0.00 ± 0.00**		4.04 ± 10.20	0.0	41.7	0	56
balance-scale	3	625	4	**8.81 ± 0.95**	15.87 ± 1.23	•	20.68 ± 17.84	1.0	92.8	23	151
balloons	2	16	4	**12.50 ± 12.50**	25.00 ± 17.68		36.79 ± 15.19	0.0	81.3	7	159
blood	2	748	4	**24.20 ± 3.47**	25.00 ± 1.75		24.17 ± 4.35	19.7	62.6	137	41
breast-cancer-wisc	2	699	9	**2.71 ± 1.17**	2.86 ± 0.99		6.54 ± 7.74	2.6	34.5	1	176
breast-cancer-wisc-diag	2	569	30	**2.46 ± 1.06**	3.87 ± 1.27		7.24 ± 8.14	1.8	37.3	10	162
breast-cancer-wisc-prog	2	198	33	**15.31 ± 1.77**	17.35 ± 2.28		24.53 ± 4.36	17.2	44.9	0	178
breast-tissue	6	106	9	**28.85 ± 11.05**	**28.85 ± 5.77**		39.08 ± 15.35	20.2	83.1	33	144
car	4	1728	6	**0.87 ± 0.60**	1.39 ± 0.33		14.01 ± 13.27	0.8	98.3	1	177
cardiotocography-10clases	10	2126	21	13.14 ± 1.54	**12.05 ± 1.15**	○	31.68 ± 20.22	11.5	84.5	4	170
cardiotocography-3clases	3	2126	21	6.12 ± 0.21	**5.18 ± 0.54**	○	12.82 ± 9.35	4.4	93.7	10	165
congressional-voting	2	435	16	**39.91 ± 2.29**	**39.91 ± 2.38**		39.58 ± 3.97	36.8	84.4	131	44
conn-bench-sonar-mines-rocks	2	208	60	**13.94 ± 2.50**	14.90 ± 3.43		25.42 ± 8.74	9.6	53.4	12	166
conn-bench-vowel-deterding	11	462	11	**0.00**	1.30		30.02 ± 29.52	0.0	98.1	0	164
contrac	3	1473	9	49.18 ± 2.60	**48.37 ± 2.31**		50.41 ± 5.55	42.8	68.5	96	78
dermatology	6	366	34	2.75 ± 0.55	**2.47 ± 0.91**		13.81 ± 20.13	1.4	69.6	30	140
echocardiogram	2	131	10	17.42 ± 2.51	**15.15 ± 2.14**		18.49 ± 5.74	12.3	46.2	106	68
ecoli	8	336	7	14.58 ± 2.96	**12.50 ± 2.15**		22.39 ± 12.92	9.1	79.5	50	123
energy-y1	3	768	8	**2.86 ± 1.07**	3.26 ± 1.30		14.05 ± 14.03	2.2	94.5	6	170
energy-y2	3	768	8	**9.24 ± 1.30**	9.64 ± 0.94		15.74 ± 12.43	6.6	95.4	39	136
fertility	2	100	9	**11.00 ± 1.73**	**11.00 ± 1.73**		14.22 ± 5.65	10.0	54.0	1	174
glass	6	214	9	25.94 ± 1.56	**24.06 ± 5.72**		39.01 ± 11.25	21.5	68.1	14	163
haberman-survival	2	306	3	**29.61 ± 2.18**	33.55 ± 1.47		27.43 ± 3.63	22.9	51.4	151	26
heart-cleveland	5	303	13	**41.45 ± 3.89**	42.76 ± 2.87		44.04 ± 4.49	35.2	80.3	38	134
heart-hungarian	2	294	12	**16.10 ± 3.54**	18.84 ± 3.27	•	20.04 ± 5.15	13.4	36.1	25	153
heart-switzerland	5	123	12	**56.45 ± 3.61**	59.68 ± 2.79		62.00 ± 5.77	46.8	87.1	24	149
heart-va	5	200	12	**67.00 ± 3.00**	67.50 ± 4.56		68.19 ± 3.83	60.0	77.5	68	103
hepatitis	2	155	19	**17.95 ± 3.14**	18.59 ± 2.13		19.97 ± 5.96	10.3	69.2	54	123
hill-valley-noisy	2	606	100	**6.93**	50.83		45.91 ± 7.53	25.7	93.9	0	176
ilpd-indian-liver	2	583	9	29.79 ± 1.03	**29.28 ± 2.44**		30.08 ± 5.18	22.4	70.5	115	60
ionosphere	2	351	33	**5.11 ± 1.70**	7.10 ± 1.68		14.05 ± 9.58	4.5	64.2	3	173
iris	3	150	4	**2.70 ± 1.91**	4.73 ± 2.24		10.61 ± 17.57	0.7	99.3	29	147
led-display	10	1000	7	27.30 ± 1.77	**27.20 ± 1.47**		39.76 ± 22.15	25.2	91.2	37	135
lenses	3	24	4	**16.67 ± 16.67**	**16.67 ± 16.67**		26.02 ± 13.60	4.2	83.3	30	119
letter	26	20000	16	**2.27 ± 0.07**	3.55 ± 0.14	•	37.28 ± 32.22	2.6	96.1	0	163
libras	15	360	90	**11.39 ± 3.46**	20.00 ± 2.22	•	42.91 ± 25.55	10.8	93.4	1	176
low-res-spect	9	531	100	**7.52 ± 0.53**	8.08 ± 0.98		19.99 ± 12.21	6.6	62.0	1	176
magic	2	19020	10	**12.31 ± 0.19**	12.76 ± 0.26	•	19.98 ± 6.75	11.7	41.4	7	159
miniboone	2	130064	50	**6.13 ± 0.07**	6.32 ± 0.08	•	17.41 ± 15.01	6.2	71.6	0	132
musk-1	2	476	166	**11.55 ± 1.82**	11.97 ± 4.88		20.59 ± 9.65	6.3	56.6	29	148
musk-2	2	6598	166	2.96 ± 0.20	**2.29 ± 0.16**	○	7.50 ± 7.94	0.2	73.5	38	134
nursery	5	12960	8	**0.15 ± 0.02**	0.34 ± 0.12	•	16.15 ± 21.35	0.0	76.7	3	157
oocytes_merluccius_nucleus_4d	0	1022	41	**15.59 ± 2.36**	22.45 ± 3.67	•	27.33 ± 10.82	14.0	91.7	2	175
oocytes_merluccius_states_2f	0	1022	25	**6.76 ± 0.98**	7.75 ± 0.85	•	14.18 ± 12.19	6.0	99.7	1	176
oocytes_trisopterus_nucleus_2f	0	912	25	**14.91 ± 1.24**	19.41 ± 1.62	•	28.79 ± 12.16	13.2	90.2	5	171
oocytes_trisopterus_states_5b	0	912	32	**6.36 ± 1.30**	7.46 ± 0.44		15.58 ± 12.61	4.9	100.0	12	163
optical	10	1797	62	2.62	**2.56**		26.67 ± 29.52	1.3	90.1	5	163
ozone	2	2536	72	2.96 ± 0.13	**2.92 ± 0.08**		5.02 ± 6.92	2.6	48.9	84	72
page-blocks	5	5473	10	2.87 ± 0.35	**2.76 ± 0.39**		5.93 ± 5.55	2.5	59.7	20	148
parkinsons	2	195	22	**6.63 ± 3.02**	10.71 ± 2.65	•	14.94 ± 7.27	5.6	62.2	8	169
pendigits	10	3498	16	**3.20**	4.35		25.31 ± 28.39	2.2	89.7	16	157
pima	2	768	8	**24.48 ± 1.61**	25.39 ± 1.00		25.73 ± 4.05	21.0	41.8	85	87
planning	2	182	12	32.22 ± 3.69	**31.67 ± 1.84**		32.32 ± 5.57	27.2	58.8	123	55
plant-margin	100	1600	64	**11.06 ± 0.48**	14.44 ± 1.30	•	50.61 ± 31.22	12.8	99.0	0	163
plant-shape	100	1600	64	**24.31 ± 0.89**	34.94 ± 1.79	•	62.16 ± 23.43	27.7	99.4	0	161
plant-texture	100	1599	64	**14.19 ± 0.84**	16.63 ± 1.35	•	49.80 ± 30.84	13.4	99.1	2	156
ringnorm	2	7400	20	**2.24 ± 0.36**	4.38 ± 0.40	•	16.09 ± 14.33	1.3	50.5	25	149
seeds	3	210	7	5.29 ± 2.50	**4.81 ± 2.15**		14.02 ± 16.34	2.8	87.0	21	146
semeion	10	1593	256	4.96 ± 1.44	**4.65 ± 1.30**		30.74 ± 27.22	3.6	89.9	9	164
spambase	2	4601	57	**4.02 ± 0.34**	4.76 ± 0.22	•	12.89 ± 9.73	3.9	43.6	1	170
spect	2	186	22	31.72	**25.81**		42.88 ± 6.07	27.8	92.5	6	170

Data set	K	N	D	CCF	TREEBAGGER		Average	Best	Worst	N_B	N_W
spectf	2	187	44	**8.02**	**8.02**		17.44 ± 21.91	7.5	94.1	4	128
statlog-image	7	2310	18	**1.39 ± 0.49**	2.04 ± 0.72	•	18.51 ± 25.22	1.4	85.9	0	176
statlog-landsat	6	2000	36	**9.10**	**9.10**		24.28 ± 19.65	8.1	78.9	6	166
statlog-shuttle	7	14500	9	0.03	**0.01**		6.61 ± 8.77	0.0	57.6	0	159
statlog-vehicle	4	846	18	**17.65 ± 2.71**	24.64 ± 1.74	•	34.61 ± 16.17	14.9	74.4	10	168
steel-plates	7	1941	27	**21.24 ± 0.87**	21.34 ± 0.83		36.40 ± 16.11	19.6	92.0	4	172
synthetic-control	6	600	60	**0.83 ± 0.73**	1.50 ± 1.09		18.19 ± 26.13	0.3	87.3	5	171
trains	2	10	29	**12.50 ± 21.65**	**12.50 ± 21.65**		31.89 ± 17.36	0.0	87.5	7	131
twonorm	2	7400	20	**2.11 ± 0.40**	2.72 ± 0.22	•	10.44 ± 13.71	2.0	50.1	2	145
vertebral-column-2clases	2	310	6	**16.23 ± 1.95**	**16.23 ± 3.84**		19.85 ± 6.46	12.6	67.8	57	120
vertebral-column-3clases	3	310	6	**13.96 ± 3.36**	15.91 ± 2.96		23.00 ± 11.63	12.6	67.8	7	170
wall-following	4	5456	24	2.93 ± 0.45	**0.46 ± 0.20**	○	21.40 ± 20.01	0.1	76.7	47	126
waveform	3	5000	21	**13.70 ± 0.93**	15.28 ± 0.99	•	23.99 ± 14.81	12.9	74.9	29	145
waveform-noise	3	5000	40	**12.78 ± 0.51**	13.88 ± 0.72	•	24.38 ± 14.75	12.6	76.3	1	174
wine	3	178	13	**0.00 ± 0.00**	1.14 ± 1.14		9.95 ± 16.15	0.0	98.3	0	176
wine-quality-red	6	1599	11	**29.94 ± 1.08**	30.88 ± 1.66		44.48 ± 12.26	31.0	98.1	0	177
wine-quality-white	7	4898	11	**30.29 ± 0.12**	31.58 ± 0.78		48.44 ± 12.39	30.9	98.2	0	173
yeast	10	1484	8	**37.60 ± 3.05**	37.80 ± 2.48		47.56 ± 10.20	36.3	70.3	3	173
zoo	7	101	16	**1.00 ± 1.73**	**1.00 ± 1.73**		13.49 ± 16.79	1.0	99.0	0	175

TABLE 8: Comparison of all classifiers on 82 UCI datasets. R is the mean rank according to error rate; E is the mean error rate (%); κ is the mean Cohen's κ [24]; E_{CCF} and κ_{CCF} are the respective values for CCFs on the datasets where the competing classifier successfully ran (note CCFs successfully ran on all datasets), N_v and N_l are the number of datasets where the CCFs κ was higher and lower than the classifier respectively, and p is the p-value for whether the CCFs κ mean is higher using a Wilcoxon signed ranks test.

Classifier	R	E	E_{CCF}	κ	κ_{CCF}	N_v	N_l	p
CCF	**28.87**	**14.08**	-	**70.67**	-	-	-	-
svmPoly_t	31.53	15.73	14.27	65.10	69.61	54	25	0.00023
svmRadialCost_t	31.84	15.33	14.27	66.55	69.61	43	36	0.11
svm_C	32	15.67	14.18	67.65	70.49	46	32	0.18
elm_kernel_m	32.19	15.20	14.54	69.01	69.75	42	36	0.16
parRF_m	33.03	15.54	14.08	67.73	70.67	52	27	0.01
svmRadial_t	33.77	15.68	14.27	65.88	69.61	50	28	0.0016
rf_caret	34.48	15.56	14.18	67.67	70.49	54	23	0.00063
rforest_R	40.70	15.82	14.18	66.67	70.49	57	20	2e-05
TreeBagger	40.91	15.75	14.08	67.51	70.67	55	23	3.5e-05
Bag_LibSVM_w	42.28	16.65	14.25	58.13	70.27	70	12	3.2e-12
C50_t	42.61	16.85	14.08	66.11	70.67	57	22	0.0004
nnet_t	42.87	18.74	14.08	64.72	70.67	54	26	0.0015
avNNet_t	43.26	18.77	14.08	64.88	70.67	50	29	0.001
RotationForest_w	44.62	16.64	14.08	65.34	70.67	64	15	7.1e-09
pcaNNet_t	45.86	19.28	14.08	63.83	70.67	54	25	0.00015
mlp_t	46.06	17.38	14.08	66.75	70.67	54	26	0.0016
LibSVM_w	46.50	16.65	14.08	63.80	70.67	57	21	2.9e-06
MultiBoostAB_LibSVM_w	46.90	16.82	14.25	64.47	70.27	61	17	1.8e-06
RRF_t	49.56	16.71	14.18	66.30	70.49	59	20	1.1e-05
adaboost_R	50.48	18.33	14.01	64.24	71.07	58	21	1.8e-06
RRFglobal_caret	51.88	16.83	14.18	65.97	70.49	58	20	2.7e-07
RandomForest_weka	52.66	16.75	14.24	63.42	69.64	62	15	1.6e-08
svmLinear_caret	53.14	17.96	14.27	61.51	69.61	60	19	1.3e-08
MultiBoostAB_RandomForest_weka	53.38	16.51	13.93	62.91	69.78	66	13	2.8e-09
gausssprRadial_R	53.75	18.41	14.69	61.92	70.70	62	17	1.9e-09
MultiBoostAB_MultilayerPerceptron_weka	56.49	17.20	14.08	66.29	70.67	61	18	2.3e-06
pnn_matlab	56.56	18.03	14.36	62.98	70.13	66	13	2.2e-08
mda_caret	57.04	20.96	14.08	62.25	70.67	59	20	4.3e-07
cforest_caret	58.27	19.52	14.61	59.80	69.50	70	9	1.9e-11
svmlight_C	58.35	18.46	15.80	61.29	65.70	57	21	5.2e-07
mlp_C	58.50	18.47	14.08	64.35	70.67	67	13	9.4e-09
Decorate_weka	58.69	17.87	14.12	64.58	70.56	65	14	7.1e-07
Bagging_RandomForest_weka	59.75	17.39	14.09	58.82	67.12	66	12	5.8e-11
rbfDDA_caret	59.91	19.23	15.80	60.96	66.34	67	11	8.7e-11
MultiBoostAB_PART_weka	60.27	18.08	14.08	65.01	70.67	61	18	2e-06
dkp_C	60.57	17.93	14.08	45.14	70.67	66	12	1e-10
knn_caret	60.94	18.93	14.08	61.20	70.67	65	14	7.7e-09
MultilayerPerceptron_weka	61.97	18.00	14.08	64.79	70.67	64	15	1.2e-07
glmnet_R	62	19.35	14.08	61.25	70.67	60	17	7.1e-09
multinom_caret	62.04	19.77	14.08	61.20	70.67	65	15	2.1e-09
Bagging_PART_weka	62.45	18.43	14.08	63.97	70.67	63	16	7.1e-08
rda_R	62.63	18.40	14.08	62.68	70.67	57	20	1.9e-07
knn_R	62.64	18.21	14.08	62.91	70.67	63	16	1.5e-08

Classifier	R	E	E_{CCF}	κ	κ_{CCF}	N_v	N_l	p
fda_caret	63.32	19.05	14.08	62.65	70.67	67	13	2.7e-09
elm_matlab	63.79	18.86	14.08	61.64	70.67	67	14	2e-09
SMO_weka	63.94	18.41	14.08	62.63	70.67	64	16	2.5e-08
RandomCommittee_weka	64.11	18.19	14.08	63.62	70.67	63	16	4.5e-09
MultiBoostAB_J48_weka	65.09	18.70	14.18	63.78	70.49	65	14	2e-08
mlpWeightDecay_caret	65.72	22.12	14.18	59.53	70.49	64	16	4.1e-09
Bagging_RandomTree_weka	65.85	18.50	14.08	63.84	70.67	64	15	3.1e-09
pda_caret	66.80	19.59	14.08	61.04	70.67	62	17	1e-09
mlm_R	66.82	19.94	14.08	60.78	70.67	65	14	1.1e-08
ClassificationViaRegression_weka	67.05	19.50	14.08	61.09	70.67	66	14	8.8e-10
Bagging_J48_weka	67.42	19.02	14.08	62.90	70.67	66	13	2.1e-09
AdaBoostM1_J48_weka	69.14	18.42	14.18	64.49	70.49	63	16	8.7e-08
treebag_caret	69.31	18.82	14.18	62.82	70.49	65	15	3.2e-09
rbf_caret	69.49	22.06	14.08	58.67	70.67	65	15	6e-09
SimpleLogistic_weka	69.76	20.26	14.08	58.47	70.67	66	14	7.2e-11
fda_R	70.26	20.09	14.08	60.35	70.67	63	16	4.4e-09
ldaBag_R	70.31	20.21	14.08	60.00	70.67	62	16	2e-09
gcvEarth_caret	70.46	20.42	14.08	60.38	70.67	66	14	1.1e-10
lda_R	70.64	20.21	14.08	60.22	70.67	63	16	3.2e-09
lssvmRadial_caret	72.38	19.13	14.51	62.62	69.66	69	10	4e-09
LibLINEAR_weka	72.68	20.36	14.08	60.29	70.67	69	11	1.7e-11
lda2_caret	72.76	20.19	14.08	59.75	70.67	67	13	2.1e-10
Bagging_Logistic_weka	73.91	19.70	13.96	60.82	70.61	67	13	1.2e-10
MultiBoostAB_RandomTree_weka	74.09	19.04	14.08	62.81	70.67	69	11	2.8e-10
Logistic_weka	75.35	20.29	13.96	59.52	70.61	69	11	1.1e-11
MultiBoostAB_REPTree_weka	75.37	19.99	14.08	61.17	70.67	72	9	1.7e-11
END_weka	75.48	19.34	14.08	61.30	70.67	66	14	3.8e-10
Bagging_IBk_weka	75.65	19.74	14.08	60.75	70.67	74	7	2.2e-12
Bagging_LWL_weka	75.65	19.74	14.08	60.75	70.67	74	7	2.2e-12
Bagging_weka	75.65	19.74	14.08	60.23	70.67	74	7	1.7e-12
mda_R	76.31	20.04	14.08	59.93	70.67	68	13	1.5e-10
sda_caret	76.40	20.34	14.08	59.40	70.67	65	13	5e-11
MultiBoostAB_Logistic_weka	76.62	20.48	14.08	60.71	70.67	65	15	2e-10
svmBag_R	76.80	25.06	13.98	55.03	70.52	65	13	2.4e-09
RandomSubSpace_weka	78.20	20.71	14.08	56.89	70.67	74	5	7.3e-14
hdda_R	79.29	20.48	14.08	59.99	70.67	62	17	6e-09
lvq_caret	79.69	19.85	14.09	58.23	70.00	70	11	3.2e-11
pls_caret	79.98	24.08	14.89	54.92	68.93	68	12	9.4e-12
ctreeBag_R	80.06	21.01	14.27	56.26	69.82	72	8	7.7e-13
MultiClassClassifier_weka	81.43	21.75	14.08	58.42	70.67	68	12	2.1e-11
LogitBoost_weka	83.48	20.92	14.08	58.88	70.67	69	10	3.3e-11
C50Rules_caret	83.87	20.95	14.08	59.97	70.67	71	8	2.5e-11
JRip_caret	83.95	22.05	14.08	56.94	70.67	69	12	6.3e-12
PART_caret	84.03	20.95	14.08	57.65	70.67	71	9	1.2e-11
RBFNetwork_weka	85.81	20.79	14.14	54.81	69.84	71	7	2.5e-12
J48_caret	86.10	20.88	14.08	56.85	70.48	68	11	1e-11
C50Tree_caret	87.52	21.49	14.08	59.16	70.67	69	10	5.5e-12
IBk_weka	87.93	20.30	14.08	61.11	70.67	68	10	1.2e-10
qda_caret	89.09	21.96	14.18	55.45	70.47	71	11	8.4e-13
PART_weka	89.14	21.53	14.08	60.35	70.67	67	13	6.4e-10
IB1_weka	89.25	20.53	14.08	60.17	70.67	71	7	1.4e-11
KStar_weka	89.32	20.74	14.18	58.60	70.49	75	4	4.6e-13
NBTree_weka	89.73	21.41	14.08	58.91	70.67	69	10	2.7e-12
J48_weka	89.94	21.75	14.18	59.29	70.49	70	10	8.1e-11
Bagging_DecisionTable_weka	91.38	22.73	14.18	55.73	70.49	75	4	7.3e-14
MultiBoostAB_DecisionTable_weka	91.52	23.78	14.18	55.37	70.49	72	8	9.5e-13
obliqueTree_R	92.02	23.77	14.14	55.43	69.84	71	8	6.9e-12
AttributeSelectedClassifier_weka	92.12	22.36	14.08	56.63	70.67	71	8	2e-12
NNge_weka	93.20	21.31	14.18	58.21	70.49	73	6	1.7e-13
bagging_R	94.07	31.45	14.18	49.22	70.49	70	11	1.7e-12
rbf_matlab	94.39	26.03	16.39	51.92	65.73	66	12	1.5e-11
DTNB_weka	96.04	22.10	14.08	56.56	70.67	72	7	3.2e-12
ctree2_caret	96.23	25.83	14.18	52.85	70.49	72	10	7.9e-12
lvq_R	96.51	27.97	14.08	52.58	70.67	72	7	2.5e-12
REPTree_weka	96.69	23.05	14.08	55.64	70.67	75	6	2.3e-13
rrlda_R	97.07	24.39	14.08	56.76	70.67	69	10	1e-10
cascor_C	97.54	23.07	14.08	57.12	70.67	71	9	7e-13
ctree_caret	98.09	24.20	14.33	53.72	69.96	73	8	5.6e-12
JRip_weka	98.14	23.08	14.18	56.73	70.49	73	8	3.4e-12
mlp_matlab	98.26	27.00	14.08	48.38	70.67	74	6	1e-13
OrdinalClassClassifier_weka	98.77	24.40	14.08	56.17	70.67	71	9	6.1e-12
nbBag_R	98.81	22.94	14.17	56.08	70.48	70	11	7.7e-12

Classifier	R	E	E_{CCF}	κ	κ_{CCF}	N_v	N_l	p
Ridor_weka	99.05	21.65	14.14	56.21	69.84	72	8	5.3e-13
bdk_R	99.14	21.99	14.08	58.06	70.67	74	5	2.7e-13
Dagging_weka	99.29	24.46	14.08	50.08	70.67	76	4	3.5e-14
rpart_caret	99.90	25.03	14.08	53.93	70.67	74	8	3.4e-12
BayesNet_weka	100.64	23.16	14.08	55.20	70.67	69	10	8.1e-13
naiveBayes_R	101.61	23.50	14.08	56.55	70.67	70	9	4.7e-12
FilteredClassifier_weka	101.65	23.82	14.08	54.16	70.67	75	4	6.7e-14
plsBag_R	101.70	31.34	14.18	44.50	70.49	72	6	3.8e-13
rpart2_caret	102.34	24.06	14.08	55.35	70.48	72	10	1.8e-11
logitboost_R	102.60	24.16	14.08	64.70	70.67	67	12	1.5e-08
rpart_R	103.37	25.84	14.08	52.04	70.67	73	8	7.3e-13
slda_caret	105.58	26.13	14.08	48.75	70.67	76	3	4e-14
nnetBag_R	105.84	39.24	14.08	35.37	70.67	70	10	2.5e-12
pam_caret	107.69	25.52	14.08	46.49	70.67	78	2	1.2e-14
mars_R	108.10	35.05	14.18	49.44	70.49	73	7	1.9e-13
MultiBoostAB_NaiveBayes_weka	109.33	25.66	14.08	52.92	70.67	70	11	1.4e-12
RandomTree_weka	111.01	23.91	14.08	55.65	70.67	76	6	3.4e-14
sddaLDA_R	111.26	26.96	14.08	44.47	70.67	76	4	3.8e-14
simpls_R	112.09	37.47	14.08	42.78	70.67	71	9	3.6e-13
widekernelpls_R	112.30	36.93	14.73	41.31	69.36	71	9	2.4e-13
Bagging_NaiveBayes_weka	113.50	26.54	14.08	51.39	70.67	70	10	1.4e-12
NaiveBayes_weka	113.84	26.49	14.08	51.54	70.67	70	10	8e-13
stepQDA_caret	114.34	27.16	14.26	45.82	70.12	75	6	5.6e-14
DecisionTable_weka	114.41	27.07	14.08	50.31	70.67	76	4	3.1e-14
QdaCov_caret	114.59	26.47	14.28	50.35	70.29	77	5	9.3e-14
kernelpls_R	114.73	39.72	14.08	40.72	70.67	71	9	3.6e-13
sparseLDA_R	114.96	30.47	13.96	43.73	70.61	72	9	3.2e-13
NaiveBayesUpdateable_weka	115.50	27.73	14.08	51.54	70.67	70	10	8e-13
bayesglm_caret	116.20	42.40	14.08	34.14	70.67	72	6	4e-13
PenalizedLDA_R	116.24	32.62	14.08	42.79	70.67	66	13	2.6e-12
sddaQDA_R	116.75	29.97	14.08	41.12	70.67	77	4	4.4e-14
stepLDA_caret	117	27.88	14.08	43.57	70.48	78	3	1.3e-14
NaiveBayesSimple_weka	124.85	26.95	13.07	50.31	70.52	75	7	1.4e-13
glmStepAIC_caret	124.85	43.05	14.20	34.13	70.37	74	5	1.3e-13
LWL_weka	126.43	30.60	14.18	42.89	70.49	75	4	6.1e-14
gpls_R	126.52	45.94	14.84	33.86	69.16	71	7	2.4e-13
dpp_C	127.03	31.59	14.08	49.22	70.67	68	12	3.3e-12
AdaBoostM1_weka	128.16	37.45	14.08	36.59	70.67	75	4	3.7e-14
glm_R	130.88	51.04	14.08	31.62	70.67	72	8	2.8e-13
Bagging_HyperPipes_weka	133.59	36.56	14.08	32.96	70.67	80	1	6.5e-15
MultiBoostAB_weka	133.60	38.57	14.08	33.58	70.67	76	3	2.2e-14
MultiBoostAB_IBk_weka	133.60	38.57	14.08	31.80	70.67	76	3	2e-14
MultiBoostAB_OneR_weka	133.72	35.98	14.08	36.85	70.67	78	2	8.8e-15
Bagging_OneR_weka	133.90	36.19	14.08	35.35	70.67	78	3	8.1e-15
VFI_weka	135.01	32.76	14.08	47.06	70.67	75	6	5e-14
Bagging_DecisionStump_weka	138.01	38.98	14.08	30.20	70.67	79	3	6.6e-15
OneR_caret	138.07	37.68	14.08	38.16	70.67	77	5	1.1e-14
HyperPipes_weka	139.46	39.62	14.08	31.01	70.67	80	2	5.5e-15
OneR_weka	139.71	37.78	14.08	34.57	70.67	79	3	7.9e-15
spls_R	140.37	46.35	14.08	19.96	70.67	78	4	9.2e-15
RacedIncrementalLogitBoost_weka	140.37	44.08	14.08	16.78	70.67	80	1	6.5e-15
DecisionStump_weka	140.85	40.81	14.08	27.77	70.67	79	3	6.8e-15
ConjunctiveRule_weka	140.92	41.12	14.08	28.71	70.67	79	3	8.5e-15
Bagging_MultilayerPerceptron_weka	143.11	46.63	14.08	16.33	70.67	77	3	1.8e-14
StackingC_weka	154.88	53.05	14.10	3.43	70.62	80	1	6.2e-15
CVParameterSelection_weka	154.90	53.05	14.10	3.45	70.62	80	1	6.2e-15
Grading_weka	154.90	53.05	14.10	3.45	70.62	80	1	6.2e-15
Stacking_weka	154.90	53.05	14.10	3.45	70.62	80	1	6.2e-15
MetaCost_weka	154.94	53.16	14.08	7.26	70.67	79	2	7e-15
CostSensitiveClassifier_weka	155.02	53.13	14.08	5.78	70.67	79	2	7.5e-15
MultiScheme_weka	155.02	53.13	14.08	2.74	70.67	80	1	6.2e-15
Vote_weka	155.02	53.13	14.08	2.74	70.67	80	1	6.2e-15
ZeroR_weka	155.02	53.13	14.08	2.74	70.67	80	1	6.2e-15
ClassificationViaClustering_weka	156.78	46.81	14.08	28.61	70.67	79	2	7.8e-15